Proceedings of the 8th International Conference on Structural Dynamics, EURODYN 2011
Leuven, Belgium, 4-6 July 2011
G. De Roeck, G. Degrande, G. Lombaert, G. Müller (eds.)
ISBN 978-90-760-1931-4

The effect of structural-acoustic coupling on the active control of noise in vehicles

Jordan Cheer[1], Stephen J. Elliott[1]
[1]Institute of Sound and Vibration Research, University of Southampton, Southampton SO17 1BJ, United Kingdom
email: j.cheer@soton.ac.uk, sje@isvr.soton.ac.uk

ABSTRACT: Active noise control systems offer a potential method of reducing the weight of passive acoustic treatment and, therefore, increasing vehicles' fuel efficiency. These can be particularly cost-efficient if integrated with the entertainment system. A combined system is presented employing feedforward control of engine noise and feedback control of road noise, using a 'modal' error signal. Due to the dependence of the feedback system on the modal response of the vehicle cabin, and the influence of structural-acoustic coupling on this response, the effects of structural-acoustic coupling upon the performance of the active noise control strategies is investigated. An elemental model of structural-acoustic coupling is derived and used to simulate the change in performance of the active control systems as a result of coupling; the feedforward component is largely unaffected by structural-acoustic coupling, whilst the modal feedback performance is reduced from 11 to 8 dB attenuation in total acoustic potential energy, due to the shift in the frequency of the targeted acoustic mode. The simulation results are confirmed through experiments conducted in a structural-acoustic coupled enclosure.

KEY WORDS: Active control; Structural-acoustic coupling; Vehicle noise.

1 INTRODUCTION

The application of active noise control to vehicles has been investigated for over 20 years [1] and, consequently, a wide variety of systems have been proposed to control both road [2] and engine noise [1]. Until recently such systems were not sufficiently integrated into the vehicle's electronic systems to provide a cost effective noise control solution, however, more recent systems [3] have overcome this restriction. There has also been an increasing desire to reduce the fuel consumption of vehicles by making them lighter, which inevitably increases low frequency noise and the need for a lightweight solution such as active control.

The presented work proposes an active noise control system consisting of a feedforward element to control tonal engine noise and a modal feedback element to control road noise. The proposed hybrid system employs a single set of error microphones for the two control elements, a reference signal for the feedforward element is directly available from the ignition circuit and the car audio loudspeakers may be employed as secondary sources. The proposed system is, therefore, largely integrable to the vehicle's standard electronic system and may provide an affordable solution to low frequency noise control of both engine and road noise. However, due to the significant influence of structural-acoustic coupling upon the low frequency sound field within a car's passenger compartment [4] and the reliance of the proposed modal feedback system upon the acoustic mode shapes of the car's cabin, it is important to investigate the effect of structural-acoustic coupling upon the system's performance.

The two active noise control strategies are first introduced and then, in order to quantify their performance, an elemental model of structural-acoustic coupling is derived. This model is used to form an understanding of how non-rigid structural panels effect the response of a car cabin sized rectangular enclosure constructed from plywood. The performance of the two control strategies is then simulated in the same enclosure for the cases where it is either fully or weakly coupled. The results of these simulations are used to highlight the effect of structural-acoustic coupling upon the proposed control methods. To confirm the simulation results a car cabin mock-up constructed from plywood is used to carry out an experimental investigation of the effect of structural-acoustic coupling upon the proposed control strategies.

2 ACTIVE NOISE CONTROL STRATEGIES

2.1 *Global Feedforward Control*

Global control of enclosed sound fields has been extensively researched and a comprehensive review is provided by Nelson and Elliott [5]. In the context of noise control within vehicles global feedforward control has been used to control both engine [1] and road noise [2]. In order to control road noise it is necessary to employ a number of reference sensors, such as accelerometers, to provide the feedforward system with a reference signal; this results in an expensive system that is unsuitable for an integrable solution. Conversely, in order to control engine noise a reference signal may be obtained from either the ignition circuit, a tachometer or the Controller Area Network bus; this is achieved relatively cheaply and, therefore, provides a suitable control method.

The proposed global feedforward control strategy attempts to minimise the sum of squared pressures at a set of error sensors using a set of secondary sources that are driven by the reference signal via an adaptive filter, as shown in Figure 1 for a single secondary source. For a set of error sensors positioned

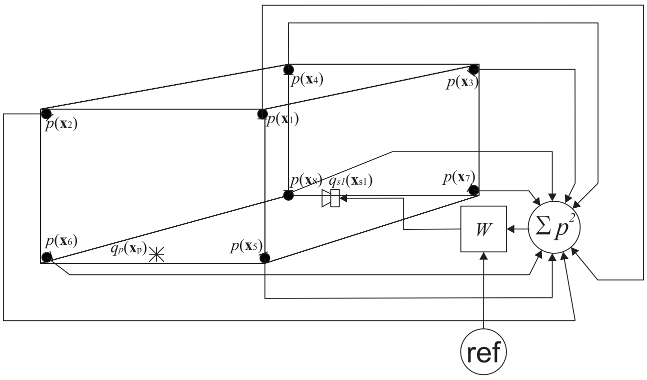

Figure 1: Global feedforward control system.

in the corners of a rectangular enclosure this is approximately equivalent to minimising the total acoustic potential energy.

The cost function that global feedforward control aims to minimise is,

$$J_p = \frac{V}{4\rho_0 c_0^2 L_e} \boldsymbol{p}_e^H \boldsymbol{p}_e \tag{1}$$

where V is the enclosure volume, ρ_0 is the air density, c_0 is the speed of sound, L_e is the number of error sensors and $\boldsymbol{p}_e$ is the column vector of error sensor pressures. The error sensor pressures result from the summation of the primary and secondary sources such that $\boldsymbol{p}_e$ can be expressed as,

$$\boldsymbol{p}_e = \boldsymbol{Z}_p \boldsymbol{q}_p + \boldsymbol{Z}_s \boldsymbol{q}_s, \tag{2}$$

where $\boldsymbol{Z}_p$ is the $(L_e \times 1)$ vector of transfer impedances between the error sensors and the primary source, $\boldsymbol{Z}_s$ is the $(L_e \times M)$ matrix of transfer impedances between the error sensors and the M secondary sources, $\boldsymbol{q}_p$ is the vector of primary source strengths, although only a single element is used here, and $\boldsymbol{q}_s$ is the column vector of secondary source strengths. The cost function J_p can thus be expressed in Hermitian quadratic form by substituting equation 2 into equation 1 and rearranging:

$$J_p = \frac{V}{4\rho_0 c_0^2 L_e} \left[\boldsymbol{q}_s^H \boldsymbol{Z}_s^H \boldsymbol{Z}_s \boldsymbol{q}_s + \boldsymbol{q}_s^H \boldsymbol{Z}_s^H \boldsymbol{Z}_p \boldsymbol{q}_p + \right. \tag{3}$$

$$\left. \boldsymbol{q}_p^H \boldsymbol{Z}_p \boldsymbol{Z}_s \boldsymbol{q}_s + \boldsymbol{q}_p^H \boldsymbol{Z}_p^H \boldsymbol{Z}_p \boldsymbol{q}_p \right]. \tag{4}$$

The vector of optimal secondary source strengths that minimises the sum of the squared error sensor pressures is then given by [5],

$$\boldsymbol{q}_{s0} = -\left[\boldsymbol{Z}_s^H \boldsymbol{Z}_s \right]^{-1} \boldsymbol{Z}_s^H \boldsymbol{Z}_p \boldsymbol{q}_p. \tag{5}$$

2.2 Modal Feedback Control

The use of feedback control offers a potential alternative to feedforward control for road noise as it does not require additional reference sensors and as such may reduce the cost of implementation. Although research into feedback control in car cabins is limited, based on its possible advantage Sano *et al* [3] have implemented a feedback control system that reduces the drumming noise at the front seats by around 10 dB, whilst avoiding enhancements at rear seats. In order to improve upon this performance and achieve global control of road noise an alternative feedback control strategy is proposed herein based on the system presented by Clark and Gibbs [6].

The feedback system presented by Clark and Gibbs employs a set of collocated transducer pairs that are spatially weighted in order to control specific acoustic modes. However, in order to employ the same error microphones for the feedforward and feedback control elements it is necessary that the sensors and actuators are not collocated, as in the feedforward control system this would create small zones of localised control around the transducer pairs. Therefore, the proposed system differs from that previously presented in its use of non-collocated sensors and actuators.

The principle of modal feedback control is to sum the pressures at a number of error sensors in order to maximise the composite, modal error signal at a specific mode and thus maximise the control of that particular mode when the modal error signal is reproduced by the secondary source. The polarity with which the error signals are summed is determined by their position relative to the nodal lines of the acoustic mode to be controlled. For the source-sensor system shown in Figure 2, in order to control the first longitudinal mode the polarity of the four error sensors in the rear corners of the enclosure is inverted before summation with the outputs of the four error sensors in the front of the enclosure.

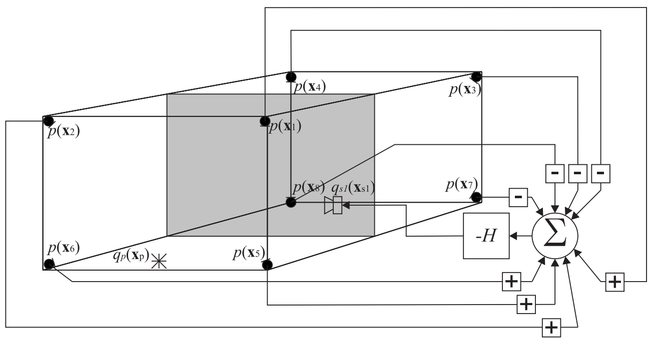

Figure 2: Modal feedback control system.

For the system presented in Figure 2 the composite error signal, p_c, can be formulated as,

$$p_c = \boldsymbol{\varphi}_L \boldsymbol{p}_e, \tag{6}$$

where $\boldsymbol{\varphi}_L$ is a $(1 \times L_e)$ vector of polarity inversions. By the action of the negative feedback the secondary source's volume velocity is given by,

$$q_s = -H p_c Y \tag{7}$$

where H is the feedback gain and Y is the volume velocity produced by the loudspeaker per unit current input and thus describes the loudspeaker response. A single degree of freedom model of the loudspeaker dynamics will be used within this paper where Y is given by,

$$Y = \frac{j\omega Bl A_d}{S(1 + j2\zeta_L \frac{\omega}{\omega_L} - (\frac{\omega}{\omega_L})^2)} \tag{8}$$

where ω is the angular frequency, Bl is the transduction coefficient, A_d is the area of the diaphragm, S is the stiffness, ζ_L is the damping ratio, and ω_L is the loudspeaker's natural frequency. Using equations 2, 6, and 7 it can be shown that the composite error signal is given by,

$$p_c = \frac{\boldsymbol{\varphi}_L \boldsymbol{Z}_p q_p}{1 + \boldsymbol{\varphi}_L \boldsymbol{Z}_s HY} \tag{9}$$

where the open-loop response is $G = \boldsymbol{\varphi}_L \boldsymbol{Z}_s HY$.

From the description of the modal feedback control system it is clear that its performance is dependent upon the modal properties of the acoustic enclosure. It is widely reported that structural-acoustic coupling has a significant effect upon the modal properties of a small enclosure such as a car cabin [4], [7] and, therefore, it is important to validate the modal feedback system in an enclosure with structural-acoustic coupling.

3 ELEMENTAL MODEL OF STRUCTURAL-ACOUSTIC COUPLING

There are a wide number of methods that have been used to model a structural-acoustic coupled system; for example, the finite element method [4], the boundary element method [8], the method based on the interaction between the uncoupled structural and acoustic modes [9], and the more recently proposed method based on the Ritz series method [10]. The elemental model derived herein follows that presented by Elliott and Johnson [11] for a vibrating structure and by Kim [12] for a structural-acoustic coupled system. It effectively implements the widely employed model of structural-acoustic coupling first proposed by Dowell and Voss [9] in physical co-ordinates. The elemental model thus lends itself to the modelling of a structural-acoustic system where there are a number of non-rigid structural components such as the multiple panels in a car cabin.

The elemental model based on the interaction of uncoupled acoustic and structural modes has been selected despite the recent work by Ginsberg [10] that has questioned the simplification employed in Dowell's model. The simplification which uses the rigid walled enclosure modes as a basis for the pressure field in the coupled enclosure means that the velocity continuity condition is not satisfied at the non-rigid boundaries. However, Ginsberg concludes that the simplified method provides accurate solutions for light fluid loading, except at frequencies below the fundamental rigid enclosure mode [10]. Additionally, Dowell's method has been widely verified experimentally and works well in most cases [13] and, therefore, will be employed herein.

The elemental model is based on dividing the system into a number of elements within which the structural and acoustic mode shape functions are approximately constant. The size of the elements must, therefore, be determined based on the frequency range of interest and the precision of the results required – for the same precision but an increased frequency of interest the element size must be reduced. At each element the response is represented by the velocity and pressure at the centre of the element. The overall system response can then be determined from the combination of elemental responses.

For an acoustic excitation within the enclosure the vector of acoustic pressures, $\boldsymbol{p}$, at the L elements on the surface of the enclosure may be related to the column vector of effective acoustic source strengths at each element, $\boldsymbol{Q}_A$, via the $(L \times L)$ uncoupled acoustic impedance matrix $\boldsymbol{Z}_A$; that is,

$$\boldsymbol{p} = \boldsymbol{Z}_A \boldsymbol{Q}_A. \tag{10}$$

The uncoupled acoustic impedance of each element in $\boldsymbol{Z}_A$ is defined as,

$$Z_A(i,j) = \frac{p(\boldsymbol{x}_i)}{Q_A(\boldsymbol{x}_j)}, \tag{11}$$

that is the ratio of the pressure produced at element i due to the effective volume velocity at element j. The acoustic pressure at the i-th element can be expressed, according to Dowell's simplification [9], as the summation over N acoustic modes of the product of the complex amplitudes of the rigid walled acoustic modes, a_n, and the mode shapes ψ_n,

$$p(\boldsymbol{x}_i) = \sum_{n=0}^{N} a_n \psi_n(\boldsymbol{x}_i). \tag{12}$$

Assuming that the effective volume velocity on the j-th element can be approximated as a point volume velocity source acting at the centre of the element, the complex amplitude of the n-th acoustic mode can be written as,

$$\begin{aligned} a_n &= \frac{\rho_0 c_0^2}{V} A_n \int_{\Delta V_j} \psi_n(\boldsymbol{x}) Q_A(\boldsymbol{x}_j) \delta(\boldsymbol{x} - \boldsymbol{x}_j) \mathrm{d}V \\ &= \frac{\rho_0 c_0^2}{V} A_n \psi_n(\boldsymbol{x}_j) Q_A(\boldsymbol{x}_j) \end{aligned} \tag{13}$$

where ΔV_j is the volume associated with the j-th element and the acoustic resonant response of the n-th mode is given by,

$$A_n = \frac{\omega}{[2\zeta_n \omega_n \omega + j(\omega^2 - \omega_n^2)]}, \tag{14}$$

where ζ_n and ω_n are the damping and natural frequency of the n-th acoustic mode respectively. Substituting equation 13 into equation 12 gives the pressure at the i-th element due to the effective source strength as,

$$p(\boldsymbol{x}_i) = \frac{\rho_0 c_0^2}{V} \sum_{n=0}^{N} \psi_n(\boldsymbol{x}_i) A_n \psi_n(\boldsymbol{x}_j) Q_A(\boldsymbol{x}_j). \tag{15}$$

Thus the uncoupled acoustic impedance between the i-th and j-th elements can be written as,

$$Z_A(i,j) = \frac{\rho_0 c_0^2}{V} \sum_{n=0}^{N} \psi_n(\boldsymbol{x}_i) A_n \psi_n(\boldsymbol{x}_j). \tag{16}$$

This may be written in vector notation as,

$$Z_A(i,j) = \boldsymbol{\psi}(\boldsymbol{x}_i)^T \boldsymbol{Z}_a \boldsymbol{\psi}(\boldsymbol{x}_j), \tag{17}$$

where $\boldsymbol{\psi}(\boldsymbol{x})$ is the $(N \times 1)$ vector of the uncoupled acoustic mode shape functions at co-ordinate position $\boldsymbol{x}$, and $\boldsymbol{Z}_a$ is the matrix of uncoupled acoustic modal impedances, which is given by the $(N \times N)$ diagonal matrix of acoustic resonant responses, $\boldsymbol{A}$, given by equation 14, multiplied by $\rho_0 c_0^2/V$. The complete matrix of uncoupled acoustic impedances may then be written as,

$$\boldsymbol{Z}_A = [\boldsymbol{\psi}]^T \boldsymbol{Z}_a [\boldsymbol{\psi}], \tag{18}$$

where $[\boldsymbol{\psi}]$ is the $(N \times L)$ matrix of uncoupled acoustic mode shape functions.

An acoustic excitation within the enclosure not only produces an acoustic pressure but also induces a source strength $\boldsymbol{Q}_S$ on the elements positioned on the non-rigid structure. These source strengths can be related to the vector of acoustic pressures via the coupled structural mobility matrix, $\boldsymbol{Y}_{CS}$; that is,

$$\boldsymbol{Q}_S = -\boldsymbol{Y}_{CS}\boldsymbol{p}. \tag{19}$$

Each element of the coupled structural mobility matrix is defined as,

$$Y_{CS}(i,j) = -\frac{Q_S(\boldsymbol{y}_i)}{p(\boldsymbol{y}_j)}, \tag{20}$$

that is the ratio of induced structural source strength at element i due to the acoustic pressure at element j. Using the relationship between the volume velocity and velocity of an element, equation 20 can be rewritten as,

$$Y_{CS}(i,j) = -\frac{\Delta S_i u(\boldsymbol{y}_i)}{p(\boldsymbol{y}_j)}, \tag{21}$$

where ΔS_i is the surface area of the i-th element. Again, according to Dowell's model [9], the vibration velocity at the i-th element may be expressed as the summation of the product of the in-vacuo complex structural mode amplitudes, b_k, and mode shapes, ϕ_k over K structural modes,

$$u(\boldsymbol{y}_i) = \sum_{k=1}^{K} b_k \phi_k(\boldsymbol{y}_i). \tag{22}$$

Based on the assumption of the elemental model that the acoustic pressure and mode shape function are constant over the j-th element, the complex amplitude of the k-th structural mode can be written as,

$$\begin{aligned} b_k &= -\frac{1}{\rho_s h S_f} B_k \int_{\Delta S_j} \mathrm{d}S \phi_k(\boldsymbol{y}_j) p(\boldsymbol{y}_j) \\ &= -\frac{1}{\rho_s h S_f} B_k \phi_k(\boldsymbol{y}_j) p(\boldsymbol{y}_j) \Delta S_j, \end{aligned} \tag{23}$$

where ρ_s is the panel density, h is the panel thickness, S_f is the surface area of the non-rigid structure and the structural resonant response of the k-th mode is given by,

$$B_k = \frac{\omega}{\left[2\zeta_k \omega_k \omega + j(\omega^2 - \omega_k^2)\right]}, \tag{24}$$

where ζ_k and ω_k are the damping and natural frequency of the k-th structural mode respectively. Substituting equation 23 into equation 22 gives the vibration velocity of the i-th element due to the acoustic reaction force as,

$$u(\boldsymbol{y}_i) = -\frac{1}{\rho_s h S_f} \sum_{k=1}^{K} \phi_k(\boldsymbol{y}_i) B_k \phi_k(\boldsymbol{y}_j) \Delta S_j p(\boldsymbol{y}_j). \tag{25}$$

Therefore, the coupled structural mobility can be written as,

$$Y_{CS}(i,j) = \frac{1}{\rho_s h S_f} \sum_{k=1}^{K} \Delta S_i \phi_k(\boldsymbol{y}_i) B_k \phi_k(\boldsymbol{y}_j) \Delta S_j. \tag{26}$$

Once again this may be written in vector notation as,

$$Y_{CS}(i,j) = \Delta S_i \boldsymbol{\phi}_i^T \boldsymbol{Y}_s \boldsymbol{\phi}_j \Delta S_j, \tag{27}$$

where $\boldsymbol{\phi}_i$ and $\boldsymbol{\phi}_j$ are $(K \times 1)$ vectors of the uncoupled structural mode shape functions at elements i and j respectively, and $\boldsymbol{Y}_s$ is the $(K \times K)$ matrix of uncoupled structural modal mobility, which is given by the $(K \times K)$ diagonal matrix of structural resonant response terms, $\boldsymbol{B}$, given by equation 24, multiplied by one over the mass of the panel. The complete matrix of coupled structural mobilities may then be written as,

$$\boldsymbol{Y}_{CS} = \boldsymbol{S}[\boldsymbol{\phi}]^T \boldsymbol{Y}_s [\boldsymbol{\phi}] \boldsymbol{S}, \tag{28}$$

where $[\boldsymbol{\phi}]$ is the $(K \times L)$ matrix of uncoupled structural mode shape functions and $\boldsymbol{S}$ is the $(L \times L)$ diagonal matrix of element areas, ΔS_l.

Since the effective source strength, $\boldsymbol{Q}_A$, is equal to the sum of the excitation source strength, $\boldsymbol{Q}$, and the induced source strength, $\boldsymbol{Q}_S$, the acoustic pressure and induced structural velocity can be expressed using equations 10 and 19 as,

$$\boldsymbol{p} = [\boldsymbol{I} + \boldsymbol{Z}_A \boldsymbol{Y}_{CS}]^{-1} \boldsymbol{Z}_A \boldsymbol{Q} \tag{29}$$

and

$$\boldsymbol{u} = -[\boldsymbol{\phi}]^T \boldsymbol{Y}_s [\boldsymbol{\phi}] \boldsymbol{S} [\boldsymbol{I} + \boldsymbol{Z}_A \boldsymbol{Y}_{CS}]^{-1} \boldsymbol{Z}_A \boldsymbol{Q} \tag{30}$$

respectively. Equations 29 and 30 may be used to describe the physical response of the structural-acoustic coupled system under direct acoustic excitation. It is important to note that the structural-acoustic system is said to be weakly coupled – i.e. the acoustic and structural systems do not interact – if the terms in square brackets in equations 29 and 30 are approximately equal to the identity matrix.

4 SIMULATIONS

The properties of the rectangular enclosure that will be investigated using the elemental model of structural-acoustic coupling are detailed in Table 1. The properties of the non-rigid panels, which are assumed to be simply supported, have been chosen to be typical of plywood, which will be employed in the later experimental study. The acoustic damping has been chosen to be typical of a small car interior [4]. The simulated responses have been generated using 100 acoustic modes and 63 structural modes per non-rigid panel. The elemental spacing has been set such that there are 6 points per wavelength at the maximum frequency of interest – 500 Hz – which results in a total of 2904 points evenly distributed throughout the enclosure.

The change in the acoustic response, or the change in the performance of the active control strategies may be investigated using the total acoustic potential energy, which can be estimated as,

$$E_p \approx \frac{V}{4\rho_0 c_0^2 L} \boldsymbol{p}^H \boldsymbol{p}. \tag{31}$$

The change in structural response due to structural-acoustic coupling may be evaluated using the total structural kinetic energy over all non-rigid panels, which can be approximated as,

$$E_k \approx \frac{\rho_s h}{4 L_s} \boldsymbol{u}^H \boldsymbol{u}, \tag{32}$$

Table 1: Enclosure properties

Property	Value
Enclosure length, L_1	2.4 m
Enclosure width, L_2	1.2 m
Enclosure height, L_3	1.1 m
Acoustic damping ratio, ζ_n	0.1
Young's Modulus, E	5×10^9 Nm^{-2}
Panel Thickness, h	12 mm
Poisson's ratio, v	0.3
Panel density, ρ_s	465 kgm^{-3}
Structural damping ratio, ζ_k	0.05

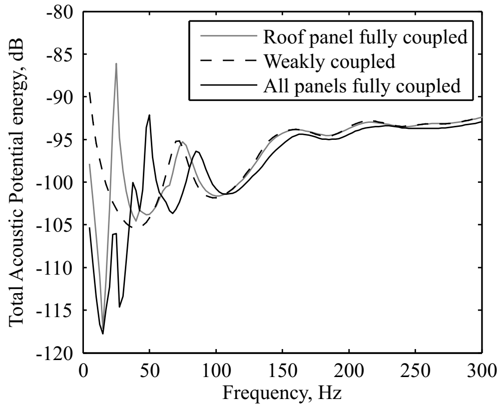

(a) Total acoustic potential energy.

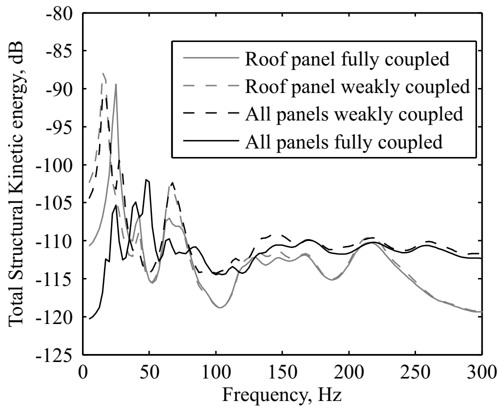

(b) Total structural kinetic energy.

Figure 3: Simulation results for acoustic enclosure with non-rigid roof panel and all non-rigid panels when excited by a single acoustic monopole source with 1×10^{-5}m^{3}s^{-1} volume velocity for the weakly coupled and fully coupled analyses.

where L_s is the number of elements that are positioned on the structure.

4.1 Acoustic excitation of the coupled system

For excitation by a monopole source with a volume velocity of 1×10^{-5} m^{3}s^{-1} positioned in the corner of the enclosure Figure 3 shows the total acoustic potential energy and the total structural kinetic energy up to 300 Hz for the weakly coupled solution, and the fully coupled solution with a non-rigid roof panel and with all panels non-rigid. From Figure 3a it can be seen that the acoustic potential energy is only significantly affected at frequencies below around 100 Hz for the non-rigid roof panel case and 200 Hz for the all panel case.

Comparing the acoustic potential energy in Figure 3a for the fully coupled system with a non-rigid roof panel to the weakly coupled system shows that the compliant mode is shifted to a lower frequency, whilst the first longitudinal mode is shifted from 71 Hz for the weakly coupled system to 75 Hz for the fully coupled system. This effect is due to interaction between acoustic and structural modes [14][4].

For the compliant acoustic mode the frequency shift is related to the interaction with the first structural mode at 16 Hz. In this case the structural mode is said to be stiffness-controlled; that is, it is predominantly excited by the acoustic response above the acoustic mode's natural frequency. This means that the structural mode increases the effective stiffness of the acoustic mode and causes its resonance frequency to reduce. A reciprocal effect also occurs as the acoustic mode increases the effective mass of the structural mode and causes its resonance to shift from 16 Hz to 26 Hz; this can be seen in Figure 3b.

The shift in the resonant frequency of the first longitudinal mode for the fully coupled analysis with a non-rigid roof panel is a result of its interaction with the $(4,1)$ structural mode at 65 Hz. This interaction causes an increase in the effective stiffness of the enclosure mode and thus an increase in its resonance frequency. The reciprocal effect causes the structural resonance to reduce in frequency, which can again be seen in Figure 3b.

From the presented observations it can be seen that interactions between two modes cause their natural frequencies to separate. The degree of interaction between structural and acoustic modes, however, is dependent upon two measures: the first is the geometric coupling, which is given by the integral of the structural and acoustic mode shape functions over the surface of the non-rigid structure; the second is the proximity of the two natural frequencies and the bandwidths of the two modes. For example, while the geometric coupling between the first longitudinal acoustic mode and the $(2,1)$ structural mode is higher than for the $(4,1)$ structural mode, its natural frequency is more than an octave below the acoustic mode's and, therefore, has no effect upon the acoustic mode. The condition for a well-coupled mode in terms of the natural frequencies and bandwidths is given by Fahy [15],

$$2|\omega_n - \omega_k| < (\Delta\omega_n + \Delta\omega_k) \tag{33}$$

where $\Delta\omega_n$ and $\Delta\omega_k$ are the bandwidth of the n-th acoustic and k-th structural modes respectively.

In addition to the variation in the natural frequencies due to the effects of coupling, a variation in the mode shape can also be expected; this is of particular importance to the modal feedback control strategy. For the $(1,0,0)$ acoustic mode the pressure distribution over a cross-section in the x_1–x_3 plane through the centre of the enclosure is presented in Figure 4. From this plot it can be seen that there is little displacement in the position of the nodal line between the weakly coupled system and fully coupled system with a non-rigid roof panel. It can, however, be seen that the fully-coupled system does result in some variation in the pressure distribution away from the nodal line; this may effect the performance of the modal feedback control system.

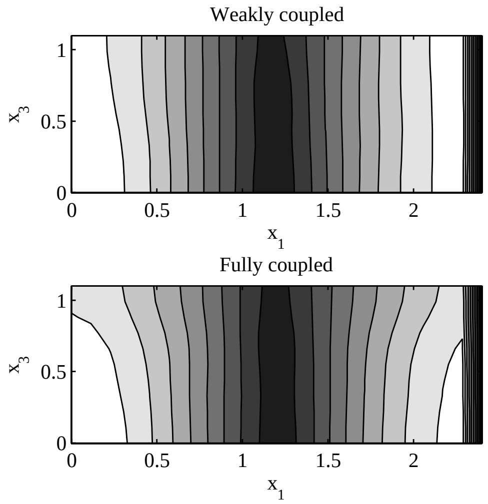

Figure 4: The pressure distribution over a cross-section in the x_1–x_3 plane through the centre of the enclosure for the first longitudinal mode occuring at $\sim$ 71 Hz in the weakly coupled case and $\sim$ 75 Hz in the fully coupled case with a non-rigid roof panel.

The effect of structural-acoustic coupling upon the enclosure with all non-rigid walls, which is also shown in Figure 3, is similar to that for the enclosure with a non-rigid roof panel that has been discussed in detail. However, due to the introduction of two sets of three different sized panels there is an increase in the number of structural modes, which can be seen in Figure 3b. The increase in the number of structural modes means that the interactions between different modes are difficult to attribute to a specific pair of modes. The main feature that may affect the performance of the modal feedback control strategy is the shift in the first longitudinal acoustic mode from 71 to 85 Hz, which can be seen in Figure 3a.

4.2 The effect of coupling upon active noise control

The effect of structural-acoustic coupling upon the active noise control strategies will be determined using the elemental model. For both global feedforward and modal feedback control the acoustic potential energy produced by a single primary monopole source with a volume velocity of 10^{-5} m^3s^{-1} will be controlled using a single secondary source, the sources and eight error sensors will be positioned in both cases as shown in Figures 1 and 2.

4.2.1 Global feedforward control

The optimum secondary source volume velocity to minimise the sum of the squared pressures has been calculated using equation 5 with the acoustic transfer impedance calculated according to equation 29 for the weakly (rigid walled) and fully-coupled (non-rigid walled) enclosures. Figure 5 shows the change in acoustic potential energy as a result of control for the rigid and non-rigid walled enclosures. From this plot it can be seen that, although the uncontrolled responses (sold lines) are significantly different, the responses after control (dashed lines) are almost identical.

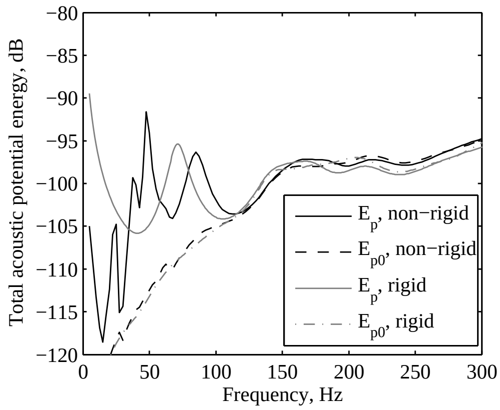

Figure 5: Total acoustic potential energy in the rigid and non-rigid enclosure when driven by a primary source alone (solid lines) and when the sum of the eight squared error sensor pressures has been minimised using a single secondary source positioned as shown in Figure 1 (dashed lines).

4.2.2 Modal feedback control

The performance of the modal feedback control strategy described in Section 2.2 has been simulated once again using the acoustic transfer impedances according to the elemental model. The gain of the feedback control system, H, has been set to ensure that the maximum enhancement of the error signal given by equation 6 is 6 dB. From Figure 6 the change in the acoustic potential energy as a result of the modal feedback control strategy is presented for the rigid and non-rigid enclosures. From this plot it can be seen that in both the rigid and non-rigid cases the feedback control strategy achieves a significant reduction around the first longitudinal mode despite the shift in its resonance frequency introduced by structural-acoustic coupling. Although the minimum of the potential energy after control is identical in both cases, the reduction at the 85 Hz target mode in the non-rigid system is 3 dB lower than that achieved at the 71 Hz mode in the rigid walled system. Additionally, enhancements in the potential energy at higher frequencies are around 1dB greater for the non-rigid walled system. Therefore, although the achievable control is reduced by the effects of structural-acoustic coupling, the energy reduction is still comparable to that achieved previously [3].

5 EXPERIMENTAL INVESTIGATION

In order to confirm the simulation results the modelled enclosure has been constructed and is pictured in Figure 7. To achieve a reasonable level of acoustic damping cotton felt was used to line the walls of the enclosure. The acoustic and structural damping of the enclosure at low frequencies were measured as 2.2% and

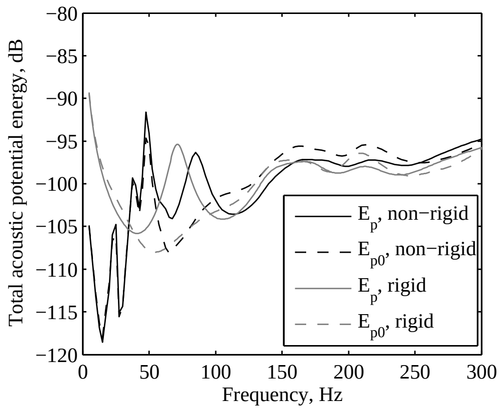

Figure 6: Total acoustic potential energy in the rigid and non-rigid enclosure when driven by a primary source alone (solid lines) and when the modal feedback control strategy using a single secondary source positioned as shown in Figure 2 has been employed (dashed lines) with a maximum error signal enhancement of 6 dB.

1.2% respectively. This is considerably lower than assumed in the simulations, however, should provide indicative results.

The acoustic response between eight microphones positioned in the enclosure's corners and both a primary and secondary source positioned as in the simulations have been measured. In both cases a Salava's volume velocity source [16] was used to excite the enclosure as this allows the acoustic transfer impedance to be measured.

Figure 7: Plywood rectangular mock-up of the car cabin with roof removed and cotton-felt damping in place.

5.1 *Global feedforward control*

The performance of the global feedforward control strategy has been calculated as in Section 4.2.1 using the measured transfer impedances instead of those from the model. Figure 8 shows the change in the acoustic potential energy estimate, J_p, as a result of feedforward control. From this plot it can be seen that significant reduction is achieved at frequencies below around 100 Hz. This is consistent with the simulations employing the fully coupled enclosure model. At the first longitudinal mode, 78 Hz in this case, J_p is reduced by approximately 24 dB compared to the 8 dB shown for the simulations in Figure 5. This difference may be partially related to the approximation of the potential energy in the experimental results, and the simulated control increases to 15 dB if J_p is calculated. The further difference in energy reduction may be attributed to the significantly lower acoustic damping in the car-cabin mock-up enclosure compared to that assumed in the model. Repeating the simulations employing damping consistent with the measured system shows a reduction comparable to the experimental results, however, these are not presented as the damping coefficients are not thought to be representative of a car cabin [4]. It is interesting to note that, in both the presented model simulations and the simulations employing the measured data, the acoustic potential energy estimate at the first longitudinal mode is reduced to around -108 dB, therefore supporting the fact that the additional reduction in the simulations employing the measured data is due to the more significant peak in the response.

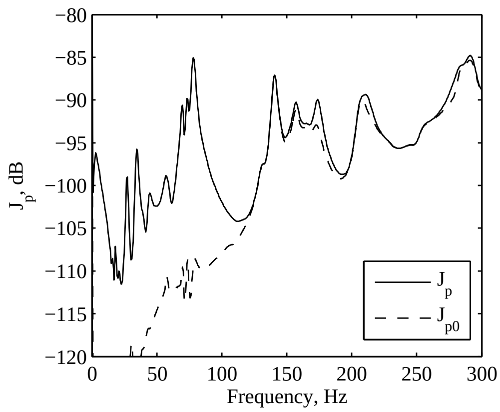

Figure 8: Estimate of total acoustic potential energy before and after simulated global feedforward control using experimentally measured responses for a single secondary source.

5.2 *Modal feedback control*

The performance of the modal feedback control strategy can also be predicted using the measured acoustic transfer impedances; however, a loudspeaker response must also be assumed and that given by equation 8 has been used here.

Figure 9 shows the acoustic potential energy estimate before and after control and from this plot it can be seen that a 9 dB reduction has been achieved at the first longitudinal mode, at 78 Hz. The maximum enhancement of 6 dB in the error signal occuring at 208 Hz has, however, resulted in a 4 dB increase in the acoustic potential energy estimate. The control around the first longitudinal mode is comparable to the 8 dB suggested by the simulations employing the fully coupled enclosure model. The prediction employing the measured results is likely to change as the damping is increased towards that assumed in the theoretical simulations; however, unlike feedforward control this relationship between damping and control is not as straightforward since increasing the acoustic damping also permits a higher feedback gain before instability.

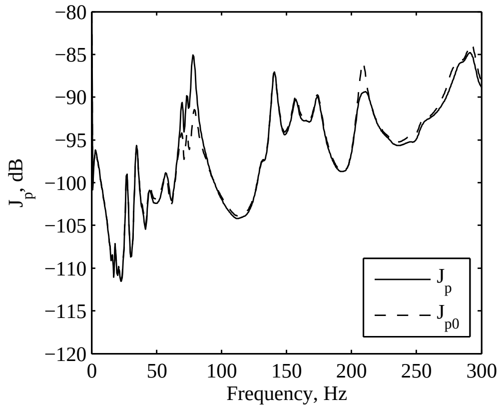

Figure 9: Estimate of total acoustic potential energy before and after simulated modal feedback control using experimentally measured responses with a single secondary source and a maximum error signal enhancement of 6 dB.

6 CONCLUSIONS

The use of integrated active noise control systems to control unwanted engine and road noise inside vehicles offers a potential method of reducing the weight of the sound package and, therefore, improving fuel efficiency. An active control system with a feedforward element to control engine noise and a feedback element to control road noise has been presented. The feedback element of the system is based on forming a modal error signal from a number of error sensors and thus via negative feedback reducing the acoustic response at a particular mode. Due to the effects of structural-acoustic coupling upon the modal response of vehicles [4] and the particular reliance of the proposed modal feedback system upon the modal response the main focus of this paper is to determine the effect of structural-acoustic coupling upon the proposed active noise control system.

An elemental model of structural-acoustic coupling is first derived based on the interaction between uncoupled acoustic and structural modes. This model is then used to investigate the effects of non-rigid panels on the acoustic response of a car cabin sized rectangular plywood enclosure. This investigation highlights that structural and acoustic modes interact only when they are both geometrically coupled, which is dependent upon their mode shapes, and have resonance frequencies that are sufficiently close. The interaction of two modes causes their resonance frequencies to move apart, however, in a complex system with many interacting modes the specific effects are more complex. For the system considered herein the main effect that may alter the performance of the feedback control system is the shift in the resonance frequency of the first longitudinal acoustic mode, which is also the targeted mode.

Using the elemental model the performance of the two active noise control systems is evaluated in both rigid and non-rigid enclosures. From these simulations it is shown that for feedforward control, despite the change in the uncontrolled responses, the controlled responses are almost identical. For the modal feedback system the reduction in acoustic potential energy at the first longitudinal mode is reduced by around 3 dB for the non-rigid enclosure compared to the rigid walled enclosure. However, the level of control is still useful.

To confirm the simulation results, measurements in a car cabin mock-up have been conducted and the performance of the control systems has been simulated using the measured transfer impedances. Despite the acoustic and structural damping being significantly lower in the mock-up compared to the model, which assumed values similar to a car, the performance of the active noise control systems are comparable to those for the simulation results.

Future work will validate the performance of the proposed control systems in an actual vehicle as well as investigate the implementation of multi-modal control using the proposed feedback strategy.

ACKNOWLEDGMENTS

This research was funded by the “European Green City Car, co2ntrol” project, part of the FP7 programme.

REFERENCES

[1] S. J. Elliott, I. M. Stothers, P.A Nelson, Malcom A. McDonald, D. C. Quinn, and Timothy J. Saunders, “The active control of engine noise inside cars,” in *Proc. INTER-NOISE 88*, Michael Bockhoff, Ed., New York, 1988, vol. 2, pp. 987–990.

[2] Trevor J. Sutton, S. J. Elliott, Malcom A. McDonald, and Timothy J. Saunders, “Active control of road noise inside vehicles,” *Noise Control Eng. J.*, vol. 42, no. 4, pp. 137–146, 1994.

[3] Hisashi Sano, Toshio Inoue, Akira Takahashi, Kenichi Terai, and Yoshio Nakamura, “Active control system for low-frequency road noise combined with an audio system,” *IEEE Trans. Speech Audio Process.*, vol. 9, no. 7, pp. 775–763, 2001, combined feedback and feedforward control in a car with predominant mode excited.

[4] D. J. Nefske, J. A. Wolf, and L. J. Howell, “Structural-acoustic finite element analysis of the automobile passenger compartment: A review of current practice,” *J. Sound Vib.*, vol. 80, no. 2, pp. 247–266, 1982.

[5] P.A Nelson and S. J. Elliott, *Active Control of Sound*, Academic Press, London, 1992.

[6] Robert L. Clark and Gary P. Gibbs, “Analysis, testing, and control of a reverberant sound field within the fuselage of a business jet,” *J. Acoust. Soc. Am.*, vol. 105, no. 4, pp. 2277–2286, 1999.

[7] A. Craggs and C. J. Buma, “The effect of an absorbent lining on the natural frequencies and modal damping factors of a small room,” *Appl. Acoust.*, vol. 28, no. 3, pp. 229 – 239, 1989.

[8] M. Tanaka and Y. Masuda, “Boundary element method applied to certain structural-acoustic coupling problems,” *Comput. Method Applied Mech.*, vol. 71, no. 2, pp. 225 – 234, 1988.

[9] E. H. Dowell and Voss H. M., “The effect of a cavity on panel vibration,” *AIAA J.*, vol. 1, no. 2, pp. 476–477, 1963.

[10] Jerry H. Ginsberg, “On dowell’s simplification for acoustic cavity-structure interaction and consistent alternatives,” *J. Acoust. Soc. Am.*, vol. 127, no. 1, pp. 22–32, 2010.

[11] S. J. Elliott and M. E. Johnson, “Radiation modes and the active control of sound power,” *J. Acoust. Soc. Am.*, vol. 94, no. 4, pp. 2194–2204, 1993.

[12] Sang-Myeong Kim, *Active control of sound in strucutral-acoustic coupled systems*, Ph.D. thesis, University of Southampton, UK, April 1998.

[13] E. H. Dowell, “Comment on “on dowell’s simplification for acoustic cavity-structure interaction and consistent alternatives”,” *J. Acoust. Soc. Am.*, vol. 128, no. 1, pp. 1–2, 2010.

[14] A. Craggs, “An acoustic finite element approach for studying boundary flexibility and sound transmission betwen irregular surfaces,” *J. Sound Vib.*, vol. 30, no. 3, pp. 343–357, 1973.

[15] F. Fahy, “Vibration of containing structures by sound in the contained fluid,” *J. Sound Vib.*, vol. 10, pp. 490–512, 1969.

[16] D.K. Anthony and S. J. Elliott, “A comparison of three methods of measuring the volume velocity of an acoustic source,” *J. Audio Eng. Soc.*, vol. 39, no. 5, pp. 355–366, 1991.